Mutation and control of the human immunodeficiency virus

Robert F. Stengel *

Department of Mechanical and Aerospace Engineering, Princeton University Princeton, P.O. Box CN5263, Princeton, NJ 08544-5263, USA

ARTICLE INFO

ABSTRACT

We examine the dynamics of infection by the human immunodeficiency virus (*HIV*), as well as therapies that minimize viral load, restore adaptive immunity, and use minimal dosage of anti-HIV drugs. Virtual therapies for wild-type infections are demonstrated; however, the HIV infection is never cured, requiring continued treatment to keep the condition in remission. With high viral turnover and mutation rates, drug-resistant strains of HIV evolve quickly. The ability of optimal therapy to contain drug-resistant strains is shown to depend upon the relative fitness of mutant strains.

© 2008 Elsevier Inc. All rights reserved.

1. Introduction

1.1. The problem

Tens of millions of people have been infected by the human immunodeficiency virus (*HIV*) since it was first recognized in the early 1980s, and more than 20 million have died from ensuing disease [1]. The virus attacks CD4-presenting cells – helper T cells, macrophages, dendritic cells, eosinophils, microglia, and natural killer cells – mainstays in the body's immune response to pathogenic attack. Without treatment, immune cells and lymphatic tissue are destroyed, and the infection evolves into acquired immune deficiency syndrome (*AIDS*), an inevitably fatal condition for all but a few [2]. While HIV itself is rarely the cause of death, the body becomes vulnerable to a host of potentially lethal opportunistic infections and malignancies, including pneumonia, tuberculosis, dementia, bacterial sepsis, lymphoma, and Kaposi's sarcoma. With multi-drug, highly active antiretroviral therapy (*HAART*), the rate of HIV progression can be dramatically slowed; fatalities brought about by the disease have plummeted since the inception of HAART.

Nevertheless, HAART is not a cure because current drug regimens cannot eliminate diverse HIV strains in a broad population [3]. Furthermore, HAART can lead to serious and discomforting side effects. Cardiovascular disease, hepatitis, liver failure, pancreas damage, glucose intolerance, kidney stones, rashes, depression, fat accumulation and redistribution, nausea, diarrhea, pain or numbness in the feet, mouth inflammation, blurred vision, headache, dizziness, anemia, weakness, insomnia, and adverse interaction with anti-HIV drugs are not uncommon [4].

There are a number of reasons why the human immunodeficiency virus cannot be defeated with current therapy. The virus targets different immune-system cell types that are capable of replicating the virus; treatments that inhibit HIV replication in one cell type may not be as effective for another. Thus, the virus is sequestered in reservoirs that are the source of latent infection. Once infected by a single HIV particle (or *virion*), an immune cell may produce over a thousand copies of the virion before the cell is destroyed; hence, unchecked infection is exponentially unstable. Long-term remission requires continued stable control over the immune cells that are vulnerable to infection for the remainder of the patient's life. There is no assurance that the last virion will not replicate unless the therapy induces stable decay to the HIV production process [5].

The pathogen is able to adapt to maintain its virulence in the presence of natural immune response and drug therapy. HIV is a retrovirus that transmits the genetic code contained in its dual strands of RNA by reverse transcription to cDNA [1]. This process is not monitored and controlled by the exonuclease proof reading that occurs in forward transcription from DNA to RNA. Thus, the DNA that the virus splices into the host cell's genome is highly variable. Many mutants of the virus are replicated, and some of these are likely to resist therapy.

In the remainder of the paper, we present a mathematical model of HIV infection with drug-resistant mutation and demonstrate the effects of mathematically optimal therapy. The virtual therapy is optimal in the sense that it minimizes the infectious viral load and count of infected helper T cells (also called T_h or CD4$^+$ cells), trading off the beneficial effects of reduced concentrations of the virus and infected cells against the adverse side effects of therapy.

* Tel.: +1 609 258 5103; fax: +1 609 258 6109.
E-mail address: stengel@princeton.edu

Coupling between wild-type (typical or most cost common) and less-fit drug-resistant HIV strains plays an important role in providing such control.

1.2. Therapy, persistence, and mutation

Because HIV has a high turnover rate, the main goal of current HIV therapy is to break the replication cycle. Fundamental damage to the immune system occurs during the first weeks of infection, when the diversity of virions is small [6]. A "hit early, hit hard" approach to therapy is more likely to minimize damage to lymphoid tissue and to eradicate a higher percentage of virulent particles than delayed treatment would [7].

With ten to a hundred million productively infected copies circulating at any given time, T_h cell infection is not only the disease's predominant feature, it is at the core of the immune system's dynamic response to HIV. Current HIV drugs enter the cells' nucleus and cytoplasm via passive diffusion, and they operate at chokepoints in the replicative sequence. *Reverse transcriptase inhibitors* (*RTIs*) are intended to prevent viral RNA from producing viral cDNA, thereby preventing a target cell's genome from being modified. The HIV's reverse transcriptase cannot distinguish between viral nucleosides and *nucleoside-analog RTIs* (*NRTIs*), which contain a chain-terminating sequence that prevents the formation of complete HIV cDNA [8]. *Non-nucleoside RTIs* (*NNRTIs*) use a different mechanism, blocking a binding pocket in the HIV reverse transcriptase to halt synthesis. *Protease inhibitors* (*PIs*) act farther downstream in the replication process, preventing protease from cleaving the long HIV peptide chain produced by translation into the smaller proteins that are essential to fusing virions with new targets. A PI does not prevent the synthesis of viral components, but it does render the components non-infectious. Dosage is a critical factor not only in treating the disease but also in causing adverse side effects and creating selective pressure for mutation. PIs are generally less toxic than RTIs, and they are less likely to select for drug-resistant mutants.

The principal failing of these drugs is that they are vulnerable to mutation in the HIV genome. The genome contains about 10^4 base pairs, and the point mutation rate is about one per 10^3–10^4 base-pair replications, or one to 10 per virion replication [7]. Given the broad nature of mutation [9], only a small percentage of mutant quasispecies are viable [10]. However, the number of new virions produced each day is large, and it is just a matter of time before strains resistant to any *monotherapy* (i.e., single-drug therapy) appear. Without therapy, wild-type strains dominate most mutant strains; however, with therapy, wild-type quasispecies are repressed, giving less-fit (but potentially lethal) mutants the opportunity to survive.

While a single point mutation in the reverse-transcriptase genomic sequence is sufficient to cause resistance to an NNRTI [11], multiple mutations are required to escape NRTIs or PIs [10,12]. Furthermore, resistance to one drug in a class (e.g., NRTI, NNRTI, or PI) can produce cross-resistance to other drugs in the same class [12]. Consequently, monotherapy is susceptible to early drug resistance. Because HAART employs several drugs of different types, many mutations are required to defeat the therapy. Adding new classes of drugs to the HAART "cocktail," such as attachment, fusion, maturation, and integrase inhibitors or adjuvant agents (which augment natural immune functions), should further increase the number of mutations required to defeat treatment. Tailoring therapeutic profiles through a better understanding of HIV-immune system dynamics can improve overall efficacy and minimize side effects [13]. Preventative vaccines are desperately sought, but there is little hope that they will be available soon [14].

2. Mathematical models and control of HIV-immune system dynamics

Mathematical models of HIV-immune system dynamics (or "host–pathogen interactions") were proposed not later than 1986 [15,16], and the disease has become the subject of intense modeling efforts. A review of all of the models is beyond the present scope; however, we direct attention to several important papers. References [3,15–35] investigate dynamic models of host–pathogen interactions for the principal virus strain, HIV-1; these papers compare and correlate response characteristics with biological and clinical observations. Consideration is given to infection in various compartments [18–20], modeling viral killing explicitly or implicitly [21], macrophage infection [22], and causes of transient viremia [3,23]. Several of the papers demonstrate computed effects of therapeutic alternatives, such as switching various drugs on or off during the course of infection [24–27] and vaccination [28]. Systems and control theories are applied to the specification of therapeutic protocols in [36–43], particularly through optimization of a treatment history or stabilization via feedback. All of these models and design studies are based on ordinary-differential equations, typically of order four or less.

2.1. Wild-type model of host–pathogen interaction

The present paper takes the fourth-order model of [[38], after [29] and [30]] as a starting point, with modifications to the ways in which control effects are expressed, with significant changes to the cost function that is minimized by optimal control, and with the addition of a drug-resistant compartment. This model contains many of the central elements of other models, and it captures the major features of HIV infection. The four elements of the initial model's state represent concentrations ($\#/mm^3$) of free, wild-type, infectious HIV particles (x_1), uninfected T_h cells (x_2), proviral infected T_h cells (x_3), and productively infected T_h cells (x_4) in the periphery, gut, and lymphoid organs.[1] The model of host–pathogen dynamics is illustrated in Fig. 1. Ovals represent elements of the state, and boxes are elements of control; arrows depict the replication cycle and dynamic interactions with the state. The model is expressed by the ordinary-differential equations,

$$\dot{x}_1 = -a_1 x_1 - a_2 x_1 x_2 (1 - u_2) + a_3 a_4 x_4 (1 - u_1) \tag{1}$$

$$\dot{x}_2 = \frac{a_5}{1 + x_1} - a_2 x_1 x_2 (1 - u_2)(1 - u_4) - a_6 x_2$$
$$+ a_7 \left(1 - \frac{x_2 + x_3 + x_4}{a_8}\right) x_2 (1 + u_3) \tag{2}$$

$$\dot{x}_3 = a_2 x_1 x_2 (1 - u_2)(1 - u_4) - a_9 x_3 - a_6 x_3 \tag{3}$$

$$\dot{x}_4 = a_9 x_3 - a_4 x_4 \tag{4}$$

The form and rationale for the dynamic equations are given in [29,30,38]. From [38], the parameter values are $a_1 = 2.4$, $a_2 = 2.4 \times 10^{-5}$, $a_3 = 1200$, $a_4 = 0.24$, $a_5 = 10$, $a_6 = 0.02$, $a_7 = 0.03$, $a_8 = 1500$, and $a_9 = 0.003$. The degree to which these equations reflect current knowledge of HIV dynamics can be assessed by referring to the prior sections of this paper. Clearly, many effects are aggregated and simplified; the core notion is that infection of T_h cells is the dominant dynamic characteristic. Explicit cytotoxic and phagocytic immune effects are not modeled but are incorporated in parameter definitions; a discussion of this assumption

---

[1] Ref. [32]] notes that protease inhibitors do not prevent the production of virions but they do render them non-infectious. Consequently, the rate of infectious virion production, $\dot{x}_1$, is reduced by PI therapy, where the PI concentration is represented by u_1 (Eq. (1)). The clinically measured total viral load following the start of PI treatment is the sum of infectious and non-infectious populations. Because the non-infectious component does not affect the T-cell population [32] and no use is made of a total viral load measurement, the non-infectious population need not be modeled here.
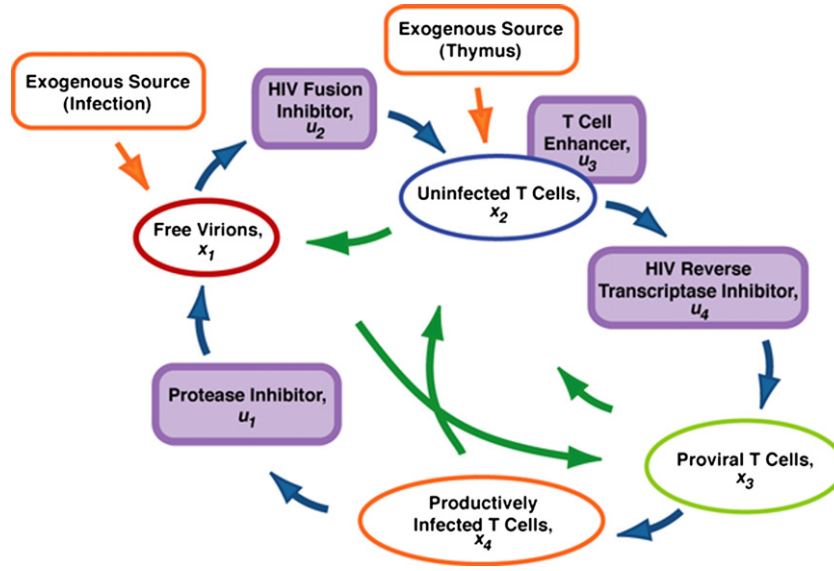
Fig. 1. Overview of the dynamic model for HIV-immune system interaction.

can be found in [21]. Eqs. (1)–(4) do not account for mutation, whose effects are considered in a later section.

The model of infection and immune response (Eqs. (1)–(4)) can be expressed in vector form as,

$$\dot{\mathbf{x}}(t) = \mathbf{f}[\mathbf{x}(t), \mathbf{u}(t)] \qquad (5)$$

where $\mathbf{x}^{\mathrm{T}}(t) = [x_1(t) x_2(t) x_3(t) x_4(t)]$ is the $(n \times 1)$ state vector and $\mathbf{u}^{\mathrm{T}}(t) = [u_1(t) u_2(t) u_3(t) u_4(t)]$ is the $(m \times 1)$ control (or therapy) vector. The control vector is different from that considered in [38]; its elements are concentrations of protease inhibitor (u_1), fusion inhibitor (u_2), T_{h} cell enhancer (u_3), and reverse transcription inhibitor (u_4). The controls either attenuate or enhance naturally occurring terms in the dynamic equations and take values in the range of $(0, 1)$. If an inhibitor (u_1, u_2, u_4) takes a value of one, it eliminates the term's effect. When the enhancer u_3 takes a value of one, the concentration-limited rate of healthy T_{h} cell production is doubled. Here, we illustrate monotherapies that employ either PIs or RTIs.

A typical untreated wild-type response is shown in Fig. 2. The initial condition is taken at a point beyond sero-conversion where the immune system is still reducing viral load [$x_1(0) = 0.049, x_2(0) =$
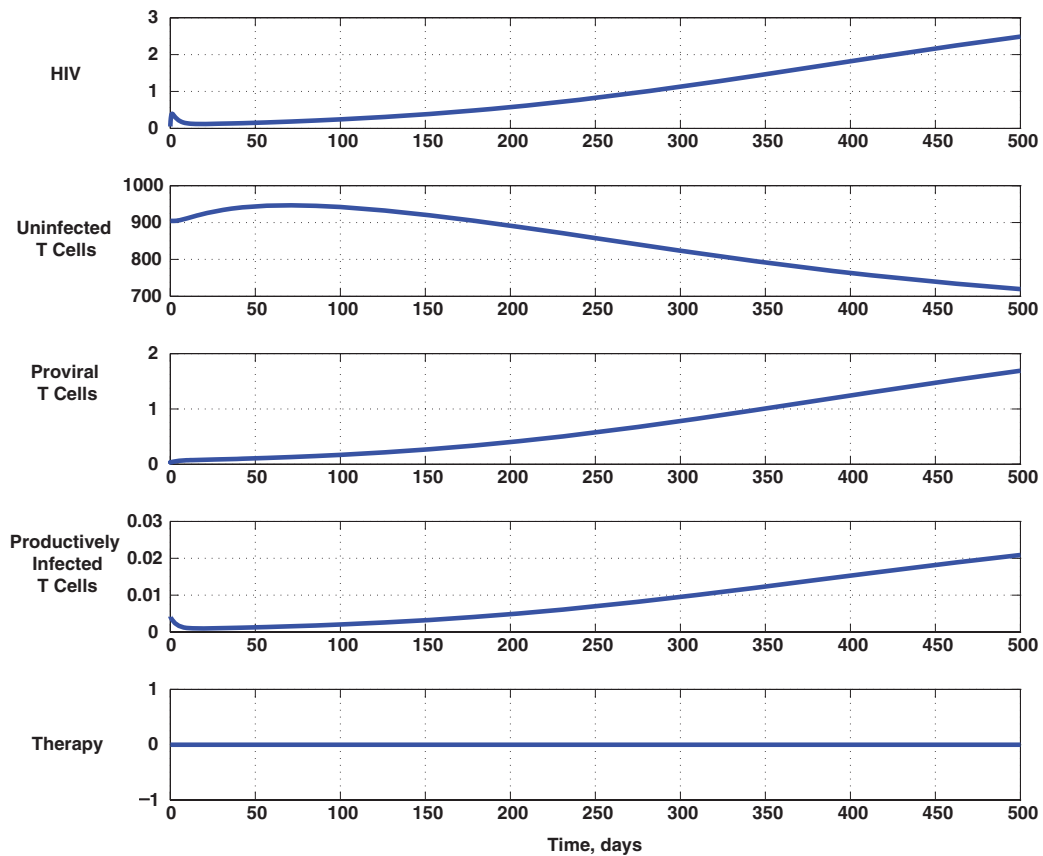

Fig. 2. Untreated response to wild-type HIV infection.

$904, x_3(0) = 0.034, x_4(0) = 0.0042$]. Uninfected T_h cell concentration is climbing (a good response), but so are the concentrations of infected cells, indicating that the HIV replication process is progressing. Over a simulated period of a year-and-a-half, the concentrations of free virions and infected T_h cells grow, while concentration of uninfected T_h cells decays. Left unchecked, the patient generally progresses to AIDS when the total T_h cell concentration falls below 200 cells per mm^3 of blood.

2.2. Optimal therapy for wild-type infection

The optimal therapeutic protocol is derived by minimizing a treatment cost function, J, that penalizes large values of HIV and infected T_h cell concentrations at the end time and during the fixed time interval $[t_o, t_f]$, as well as excessive application of therapeutic agents during the interval. The scalar cost function has terminal and integral components, and it takes the general form,

$$J[\mathbf{x}(t), \mathbf{u}(t)] = \frac{1}{2}\left\{\mathbf{x}^T(t_f)\mathbf{S}_f\mathbf{x}(t_f) + \int_{t_o}^{t_f}[\mathbf{x}^T(t)\mathbf{Q}\mathbf{x}(t) + \mathbf{u}^T(t) + \mathbf{u}^T(t)\mathbf{R}\mathbf{u}(t)]dt\right\}$$
$$= \phi[\mathbf{x}(t_f)] + \int_{t_o}^{t_f} L[\mathbf{x}(t), \mathbf{u}(t)]dt$$
(6)

The cost function for wild-type therapy is expressed as

$$J[\mathbf{x}(t), \mathbf{u}(t)] = \frac{1}{2}\left[s_{f_{11}}x_1(t_f)^2 + s_{f_{33}}x_3(t_f)^2 + s_{f_{44}}x_4(t_f)^2\right]$$
$$+ \frac{1}{2}\int_{t_o}^{t_f}[q_{11}x_1(t)^2 + q_{33}x_3(t)^2 + q_{44}x_4(t)^2 + ru_i(t)^2]dt$$
(7)

The integral and terminal populations of the virus, proviral infected T_h cells, and actively infected T_h cells are to be minimized with respect to application of the control in the time interval $[t_o, t_f]$. The diagonal matrices $\mathbf{S}$, $\mathbf{Q}$, and $\mathbf{R}$ establish relative weights that penalize variations from zero of the final state and of the state and control in $[t_o, t_f]$. The variables are squared to amplify the effects of large variations and to de-emphasize contributions of small variations. Each squared element is multiplied by a coefficient that establishes the relative importance of the factor in the treatment cost. The diagonal matrix elements (s_{ii}, q_{ii}) express allowable tradeoffs between response values, while r reflects relative financial or physiological cost, such as toxicity or discomfort. Thus, there are mechanisms for trading one variation against the others in defining the treatment protocol, balancing speed and efficacy of treatment against implicit side effects.

This cost function is significantly different from the one used in [38]; as a consequence, the results of optimization are different as well. The present cost function minimizes terminal and integral virus concentration, which is not included in the cost function of [38]; consequently, the viral concentration can be driven toward zero, which is not the case for the earlier study. T_h cell population is not included in the present cost function because forcing HIV concentration to a low value automatically restores the T_h cell population to normal levels.

The cost-function integrand, $L[\mathbf{x}(t), \mathbf{u}(t), t]$, is called the *Lagrangian* of the cost function. We adjoin the dynamic constraint to the Lagrangian in the *Hamiltonian* of the system through the $(n \times 1)$ *adjoint vector*, $\lambda(t)$:

$$H(\mathbf{x}(t), \mathbf{u}(t), \lambda(t), t) = L(\mathbf{x}(t), \mathbf{u}(t), t) + \lambda^T(t)\mathbf{f}[\mathbf{x}(t), \mathbf{u}(t)]$$
(8)
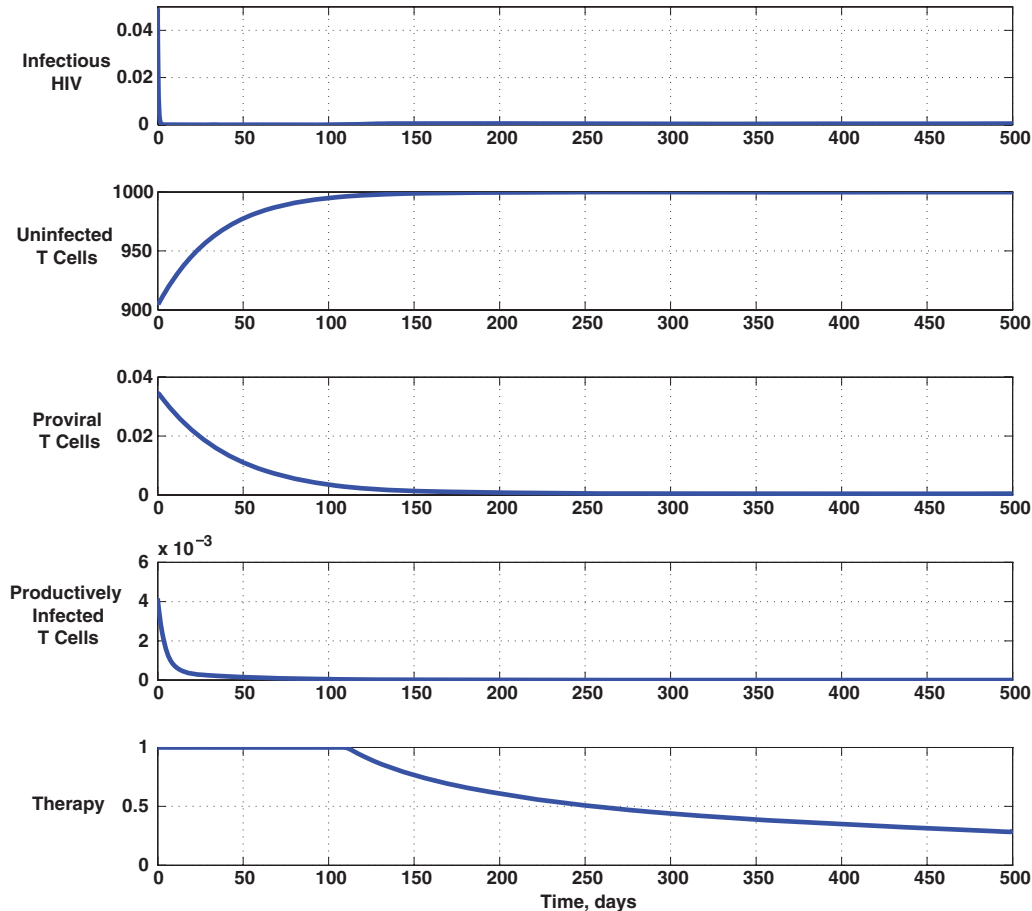
The cost function then can be expressed as

Fig. 3. Effect of optimal protease inhibitor therapy with 100% efficacy.

$$J[\mathbf{x}(t), \mathbf{u}(t)] = \phi[\mathbf{x}(t_f)] + \int_{t_o}^{t_f} \{H[\mathbf{x}(t), \mathbf{u}(t)] - \boldsymbol{\lambda}^T(t)\dot{\mathbf{x}}(t)\}\, dt \qquad (9)$$

Necessary conditions for minimizing Eq. (9) with respect to control application are expressed by the three Euler–Lagrange equations [44]:

$$\dot{\boldsymbol{\lambda}}(t) = -\left\{\frac{\partial H[\mathbf{x}(t), \mathbf{u}(t), \boldsymbol{\lambda}(t), t]}{\partial \mathbf{x}}\right\}^T = -\left[\frac{\partial L(t)}{\partial \mathbf{x}}\right]^T - \mathbf{F}^T(t)\boldsymbol{\lambda}(t) \qquad (10)$$

$$\boldsymbol{\lambda}(t_f) = \left\{\frac{\partial \phi[\mathbf{x}(t_f)]}{\partial \mathbf{x}}\right\}^T = \mathbf{S}_f \mathbf{x}(t_f) \qquad (11)$$

$$0 = \left[\frac{\partial H[\mathbf{x}(t), \mathbf{u}(t), \boldsymbol{\lambda}(t), t]}{\partial \mathbf{u}}\right]^T = \left[\frac{\partial L(t)}{\partial \mathbf{u}}\right]^T + \mathbf{G}^T(t)\boldsymbol{\lambda}(t) \qquad (12)$$

The $(n \times n)$ matrix $\mathbf{F}(t)$ and $(n \times m)$ matrix $\mathbf{G}(t)$ are symbols for the time-varying *Jacobian matrices*, $\{\partial \mathbf{f}\,[\mathbf{x}(t),\mathbf{u}(t)]/\partial \mathbf{x}(t)\}|_{\mathbf{x}(t)\,=\,\mathbf{x}^*(t),\ \mathbf{u}(t)=\mathbf{u}^*(t)}$ and $\{\partial \mathbf{f}[\mathbf{x}(t),\mathbf{u}(t)]/\partial \mathbf{u}(t)\}|_{\mathbf{x}(t)=\mathbf{x}^*(t),\ \mathbf{u}(t)=\mathbf{u}^*(t)}$, evaluated along the deterministic optimal history, $[\mathbf{x}^*(t), \mathbf{u}^*(t)]$ in $[t_o, t_f]$. The Euler–Lagrange equations include a linear, ordinary-differential equation whose integral is the *adjoint vector*, $\boldsymbol{\lambda}(t)$ (Eq. (10)), a terminal boundary condition that specifies $\boldsymbol{\lambda}(t_f)$ at the end of the interval (Eq. (11)), and a *stationarity condition* on the control throughout the interval (Eq. (12)). Eqs. (5) and (10), (11), (12) must be satisfied concurrently, specifying a *two-point boundary-value problem* that is solved numerically.

The optimizing solution is necessarily iterative because the system model is nonlinear, initial conditions are given for $\mathbf{x}$, and terminal conditions are given for $\boldsymbol{\lambda}$. The solution is begun by solving Eq. (5) with a starting estimate of the control history, $\mathbf{u}_0(t)$ in $[t_o, t_f]$. Eq. (10) is solved, integrating back from the end condition specified by Eq. (11). In general, the remaining necessary condition for optimality, Eq. (12), is not satisfied, so a *steepest-descent method* is used to generate successive approximations of the optimal control history $\mathbf{u}^*(t)$ from

$$\begin{aligned}\mathbf{u}_k(t) &= \mathbf{u}_{k-1}(t) - \varepsilon_k(t)\left\{\frac{\partial H[\mathbf{x}(t), \mathbf{u}(t), l(t)]}{\partial \mathbf{u}(t)}\right\}_{k-1}^T \\ &\equiv \mathbf{u}_{k-1}(t) - \varepsilon_k(t)[H_\mathbf{u}(t)]_{k-1}^T \end{aligned} \qquad (13)$$

where $\varepsilon_k(t)$ is a scalar gain that can be optimized from one iteration to the next [44], k is the iteration index, and $H_\mathbf{u}(t)$ is the Hamiltonian gradient with respect to control. The state variables are constrained to remain positive, and the control variable, $\mathbf{u}^*(t)$, is restricted to $(0,1)$. With no control constraint, $H_\mathbf{u}(t)$ tends to zero as $k \to \infty$, and $\mathbf{u}_k(t)$ converges to the optimal therapy, $\mathbf{u}^*(t)$. The result is a close approximation to the optimal trajectory $\mathbf{x}^*(t)$ in $[t_o, t_f]$. This approach is applied to an immune response problem in [45].

With bounded control, the steepest-descent algorithm may drive $\mathbf{u}_k(t)$ to its limiting value over some or all intervals in $[t_o, t_f]$ before $H_\mathbf{u}(t)$ comes close to zero. By Pontryagin's Principle, this bounded solution is the minimizing solution because it yields the lowest possible value of the Hamiltonian in that interval and, therefore, the lowest increment to attainable cost [44]. In all of the examples considered here, the optimal therapy starts at its maximum value, coming off the boundary as time increases. For these cases, iterative convergence is obtained after a few trials, and it is aided by choosing $\varepsilon_k(t)$ to be an increasing function of t during the early iterations.

An example based on protease inhibitor (u_1) therapy is shown in Fig. 3; for this example, $s_{f_{11}} = s_{f_{33}} = s_{f_{44}} = q_{11} = q_{33} = q_{44} = 10^3$ and $r = 0.01$. The precise values of the weighting factors are not significant; higher cost is associated with virion and infected cell concentrations, and low cost is associated with drug use. The PI is assumed to have 100% efficacy, and, as shown in Eq. (1), it has a direct effect on the rate of virion production. The maximum PI dosage is maintained for about three months, during which time the infectious viral load and infected T_h cell concentration are reduced dramatically. The uninfected T_h cell population returns to its target
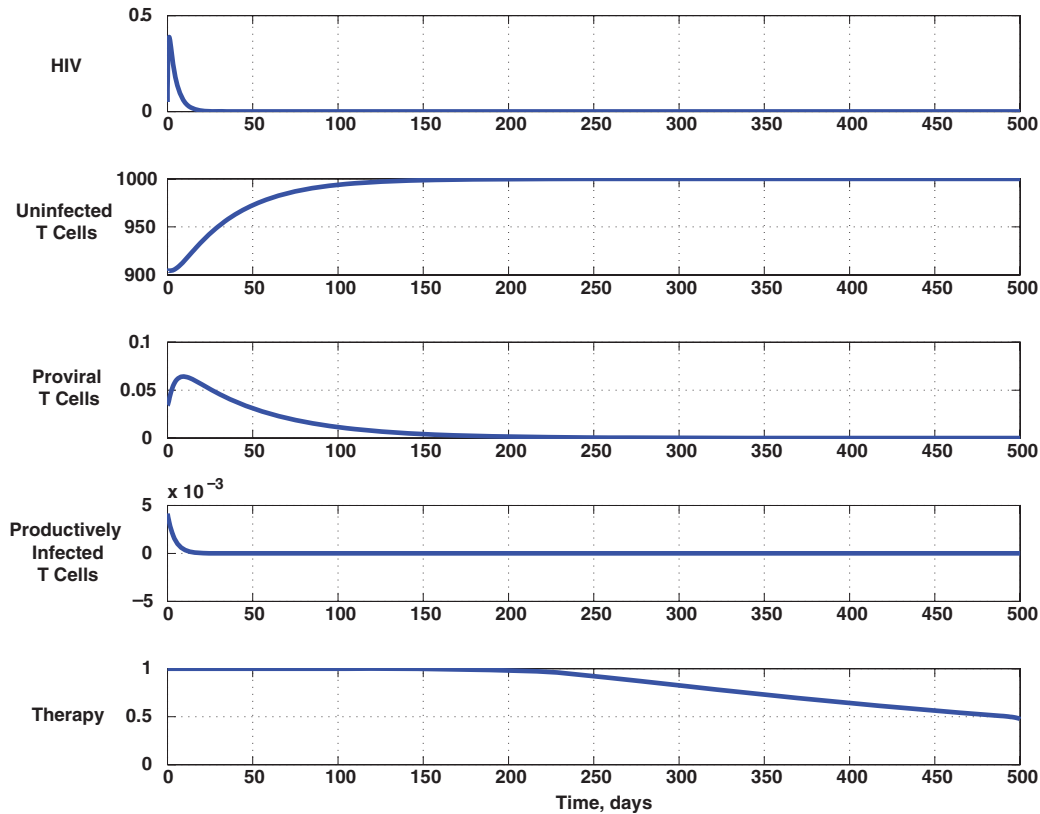

Fig. 4. Effect of optimal reverse transcriptase inhibitor therapy with 100%.

value (= 1000 cells/mm³) after five months. At the end of the period, the PI concentration is decreased toward a maintenance level. If the terminal cost and integral-state cost weights are increased by a factor of 10, the maximum therapy is applied for an additional 100 days, and the final virion and infected T_h cell concentrations are further reduced. Decreasing the maximum PI dosage to 90% (or assuming that the maximum dosage has 90% efficacy), the duration of maximum dosage is increased and the decay rate of infection is slowed. All of these results suggest that drug therapy could be reduced once the initial wild-type infection is controlled, implicitly lowering side effects and the cost of therapy.

RTI monotherapy (u_4) has an indirect effect on virion production (Eqs. (2) and (3)), reducing the rate of infected T_h cell creation which in turn reduces virion generation. The HIV concentration decreases to small values in a month, and drug dosage is reduced below the maximum after 7 months, at which point the uninfected T_h cell concentration is back to normal. These results suggest that PI and RTI therapy would be effective in controlling wild-type HIV if there were no mutation.

Although not shown, two other therapeutic effects have been calculated and are of interest. A fusion inhibitor (u_2) affects both HIV and infected T_h cell production directly (Eqs. (1)–(3)); hence, its dynamic history is similar to Figs. 3 and 4. Optimizing therapy with the cost function of Eq. (6) and a notional T_h cell enhancer (u_3) has a counter-intuitive effect: it calls for killing healthy T_h cells (through negative enhancement). The reason is that T_h cell concentration does not appear in the cost function. Because healthy T_h cells become HIV factories, the only way such a control can reduce viral and infected T_h cell concentrations is to attack healthy T_h cells.

This seemingly anomalous result suggests that temporary immune system suppression could play a role in HIV treatment, as it already does for recovery from organ transplants (suggested by Paul Shapshak, University of Miami, in personal communication). Penalizing deviation from a healthy T_h cell population in the cost function gives rise to time-variations in both viral and healthy T_h cell levels that require more study.

2.3. Model of host–pathogen interaction with wild-type and mutant infection

Regrettably, mutation does occur in HIV replication, and it leads to drug-resistant strains of the virus. The new strains do not respond to treatment, but it remains to be seen if their dynamic interactions with drug-sensitive strains can be used to good effect. To examine this possibility, we append a single mutant strain and mutantly infected T_h cell populations to our original fourth-order model:

$$\dot{x}_1 = -a_1 x_1 - a_2 x_1 x_2 (1 - u_2) + a_3 a_4 x_4 (1 - a_{10})(1 - u_1) \qquad (14)$$

$$\dot{x}_2 = \frac{a_5}{1 + x_1 + x_5} - a_2 x_1 x_2 (1 - u_2)(1 - u_4) - a_6 x_2$$
$$\quad - a_2 a_{11} x_5 x_2 + a_7 \left(1 - \frac{x_2 + x_3 + x_4 + x_6 + x_7}{a_8}\right) x_2 (1 + u_3) \qquad (15)$$

$$\dot{x}_3 = a_2 x_1 x_2 (1 - u_2)(1 - u_4) - a_9 x_3 - a_6 x_3 \qquad (16)$$

$$\dot{x}_4 = a_9 x_3 - a_4 x_4 \qquad (17)$$

$$\dot{x}_5 = a_3 a_4 a_{10} x_4 + a_3 a_4 x_7 - a_1 x_5 - a_2 a_{11} x_5 x_2 \qquad (18)$$

$$\dot{x}_6 = a_2 a_{11} x_5 x_2 - a_9 x_6 - a_6 x_6 \qquad (19)$$

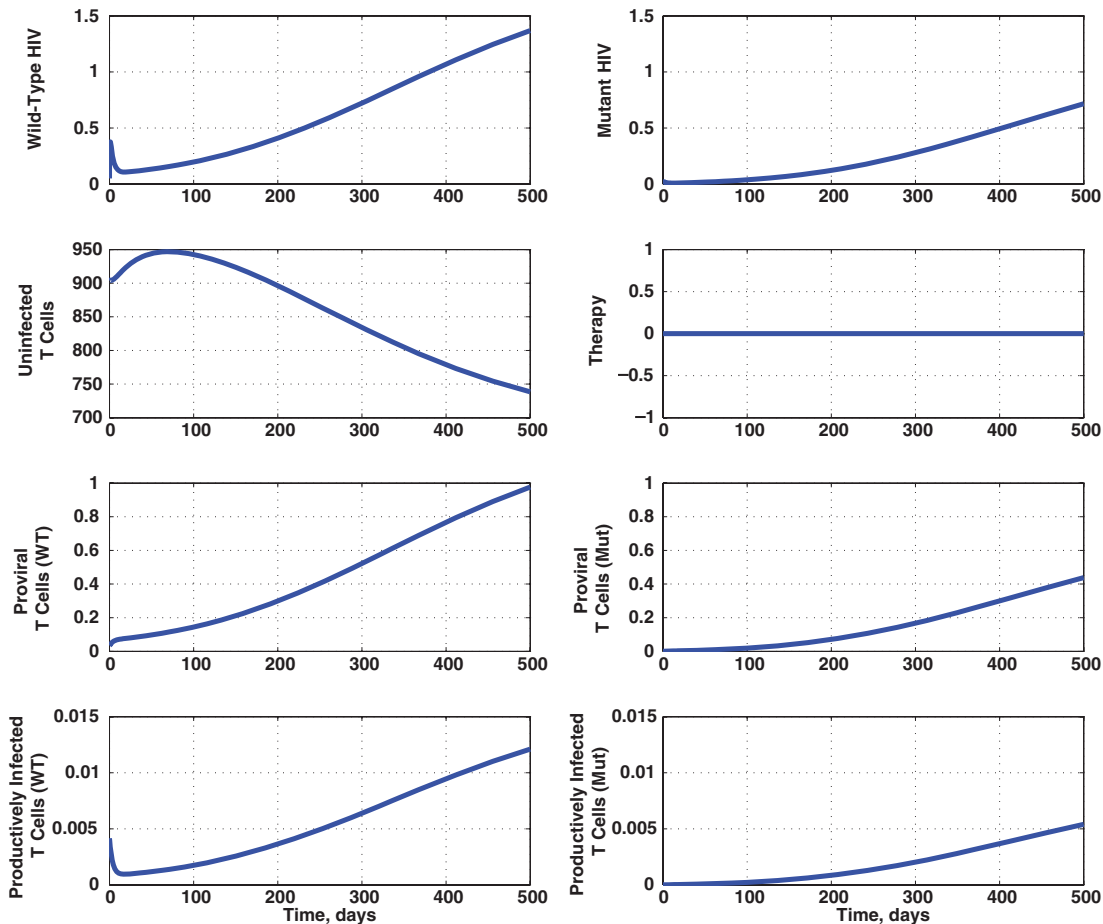$$\dot{x}_7 = a_9 x_6 - a_4 x_7 \qquad (20)$$

Fig. 5. Untreated response to wild-type and mutant infection. Mutant fitness = 90%.

The new state elements represent concentrations of the infectious, mutant HIV strain (x_5), proviral T_h cells infected by the mutant strain (x_6), and T_h cells productively infected by the new strain (x_7). The differential equations for these three variables (Eqs. (18)–(20)) are modeled after Eqs. (1), (3), and (4), but they do not contain direct effects of therapy. The rate of mutant HIV production (Eq. (18)) is proportional to the concentration of T_h cells that are productively infected by wild-type virions (x_4) and by mutant virions (x_7). The mutant compartment is coupled to the previous equations by a mutation rate term (with multiplier a_{10}), and it contains a decay term representing "fitness" that is moderated by a_{11}. The wild-type strain is assumed to have a fitness of one (after [46]), and the mutant strain has a fitness (a_{11}) less than one (else it would be a wild-type strain through evolution). The equation governing the production of healthy T_h cells (Eq. (7)) also is modified to account for the new populations of virions and infected cells. For illustrative purpose, we assume that the mutation rate is 10% ($a_{10} = 0.1$), about twice the highest value found in the literature, and we allow the mutant strain fitness to vary between 10% and 90% ($a_{11} = 0.1$–0.9).

With a mutant fitness of 90% and no therapy, both HIV strains progress, and the healthy T_h cell population decays as before (Fig. 5). The initial condition for simulation is [$x_1(0) = 0.049$, $x_2(0) = 904$, $x_3(0) = 0.034$, $x_4(0) = 0.0042$, $x_5(0) = x_6(0) = x_7(0) = 0$]. Mutant virions are initially created in T_h cells that are productively infected by the wild-type strain; as the population of T_h cells infected by the mutant strain grows, they, too, produce mutant virions. The rate of growth is about the same for wild-type and mutant strains, although the latter has lower net concentration. Reducing

the mutant fitness to 10% produces a similar result, but the mutant concentration is lower still. Throughout the simulated period, both mutant strains grow, but the wild-type strain remains responsible for the bulk of infection.

2.4. Optimal therapy for wild-type plus mutant infection

Protease inhibitor therapy is optimized for the augmented system. To illustrate the "controllability" of the mutant strain (or lack thereof), the cost function is reframed to penalize the growth of the mutant strain and its infection of T_h cells:

$$J[\mathbf{x}(t), \mathbf{u}(t)] = \frac{1}{2}\left[s_{f_{55}}x_5(t_f)^2 + s_{f_{66}}x_6(t_f)^2 + s_{f_{77}}x_7(t_f)^2\right]$$
$$+ \frac{1}{2}\int_{t_o}^{t_f}[q_{55}x_5(t)^2 + q_{66}x_6(t)^2 + q_{77}x_7(t)^2 + ru_i(t)^2]\,dt$$

(21)

Controllability is the capacity to force a dynamic system from an arbitrary initial condition to a desired final state in finite time; here, the desired final state is comprised of the populations of mutant virions and the T_h cells that they infect. A system may be controllable through dynamic coupling of system variables even though the terms in the final state are not directly affected by the control. For a system with no constraints on the control magnitude, controllability is assured if

$$c = \int_{t_o}^{t_f}[\boldsymbol{\lambda}^{\mathrm{T}}(t)\mathbf{G}(t)\mathbf{G}^{\mathrm{T}}(t)\boldsymbol{\lambda}(t)]\,dt \neq 0$$

(22)

along a typical trajectory [44]; this is the case for the HIV-immune system model and cost function. Nevertheless, because the drug
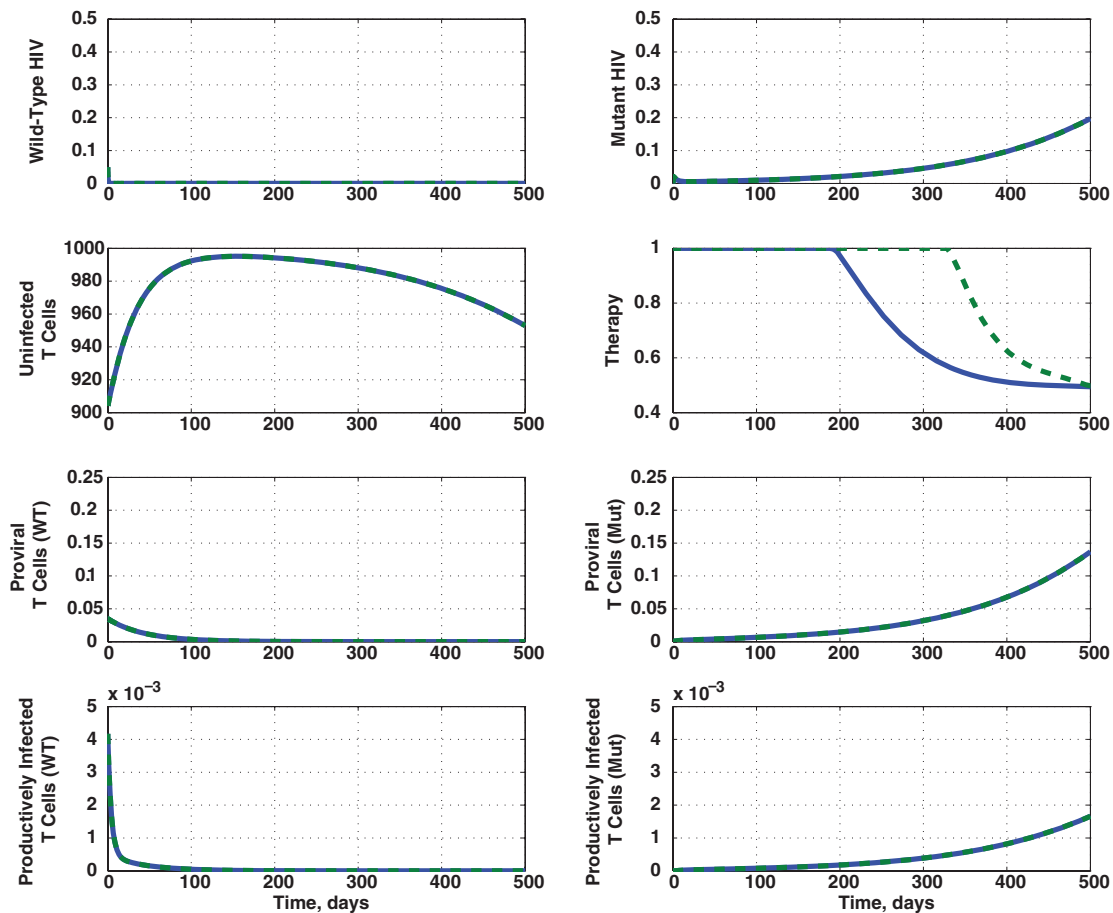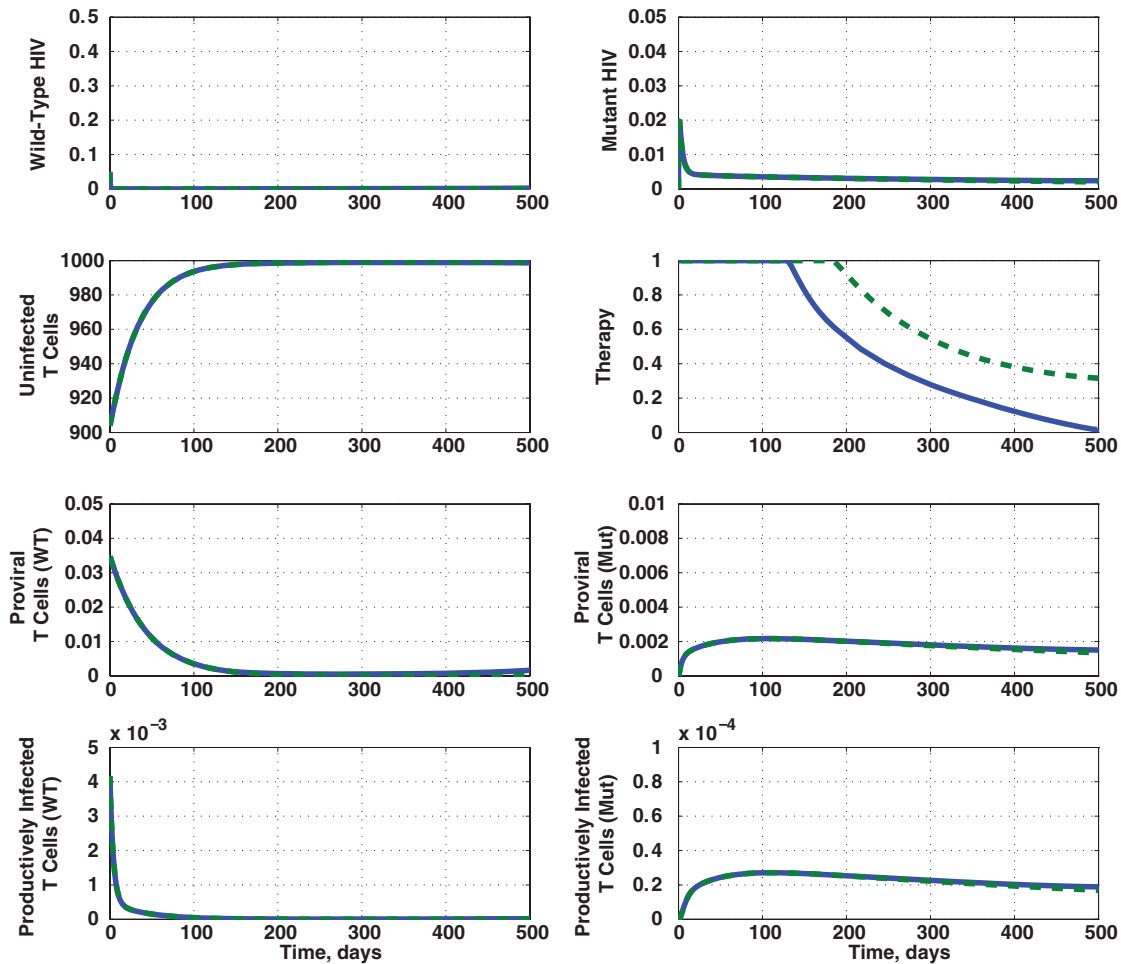

Fig. 6. Response of wild-type and mutant virus to optimal protease inhibitor therapy. Mutant fitness = 90%. $s_{f_{55}} = s_{f_{66}} = s_{f_{77}} = q_{55} = q_{66} = q_{77} = 1000$, and $r = 0.01$ (solid line), $s_{f_{55}} = s_{f_{66}} = s_{f_{77}} = q_{55} = q_{66} = q_{77} = 10000$, and $r = 0.01$ (dashed line).

Fig. 7. Response of wild-type and mutant virus to optimal protease inhibitor therapy. Mutant fitness = 60%. $s_{f_{55}} = s_{f_{66}} = s_{f_{77}} = q_{55} = q_{66} = q_{77} = 1000$, and $r = 0.01$ (solid line), $s_{f_{55}} = s_{f_{66}} = s_{f_{77}} = q_{55} = q_{66} = q_{77} = 10\,000$, and $r = 0.01$ (dashed line).

concentration is restricted to the range (0,1), control saturation may prevent the desired goal from being reached.

The cost function parameters are $s_{f_{55}} = s_{f_{66}} = s_{f_{77}} = q_{55} = q_{66} = q_{77} = 1000$, and $r = 0.01$.[2] The steepest-descent optimization is applied as before. With a mutant fitness of 90%, the PI effect on the wild-type HIV strain is similar to the unmutated case (Fig. 3). The wild-type is virtually eliminated within the first few weeks through the action of maximum drug dosage (Fig. 6), but the mutant strain grows exponentially and becomes dominant in a few weeks. The optimal therapy remains at full value for the first several months of treatment (solid curve in Fig. 6), where the integrand of Eq. (22) is large; however, the saturated control effect is not large enough to defeat the mutant virus. Beyond this point, the integrand of Eq. (22) is small, and therapy has negligible effect on the HIV population. The therapy decreases to reduce the control cost, with little impact on the infection. For $s_{f_{55}} = s_{f_{66}} = s_{f_{77}} = q_{55} = q_{66} = q_{77} = 10\,000$ (dashed curve in Fig. 6), therapy remains at its maximum value for an additional four months, although there is negligible effect on either the wild-type or mutant populations.

Reducing the mutant fitness level to 70% has little effect on the optimal PI therapy history, but the healthy T_h cell count is maintained at high levels for the period (not shown). The wild-type HIV is controlled as before, and the mutant strain grows at a much

lower rate. A further reduction in mutant fitness to 60% has a dramatic effect: the mutant concentration and its effects diminish over time (Fig. 7). The optimal dosage becomes smaller toward the end of the period. Terminal and integral-state weights of 1000 produce the solid curves in the figure, while weights of 10 000 produce the dashed curves. Only the therapy curve is clearly distinguishable between the two cases, remaining at the maximum value for an additional two months. Thus, there is a dividing point between success and failure in controlling the drug-resistant mutant strain at a fitness level between 60% and 70%.

Three phases of mutant HIV population growth are evident: initial step due to wild-type HIV and productively infected T_h cell populations, decay associated with reduction in both of these populations, and growth associated with expansion of the mutantly infected T_h cell population. If therapy does not arrest mutant virion growth before the third phase becomes dominant, the infection cannot be controlled.

It has been suggested that "start–stop therapy" or "drug holidays," in which treatment is stopped for a period of time, could control the growth of mutant strains by allowing the wild-type to reestablish itself and out-compete the mutant type for resources. Although largely discounted by clinical trials [4,47], it is interesting to compare periodic therapy with optimal therapy. The solid curve of Fig. 8 portrays the effect of PI therapy that is switched on and off every 60 days for a mutant strain with 60% fitness and terminal and integral-state weights of 10 000. The wild-type population increases during the "off" periods, and associated

---

[2] The wild-type strain is, of course, still dangerous and could be retained in the cost function; it is neglected simply to demonstrate that the wild-type is controlled in the process of attempting to control the mutant strain.
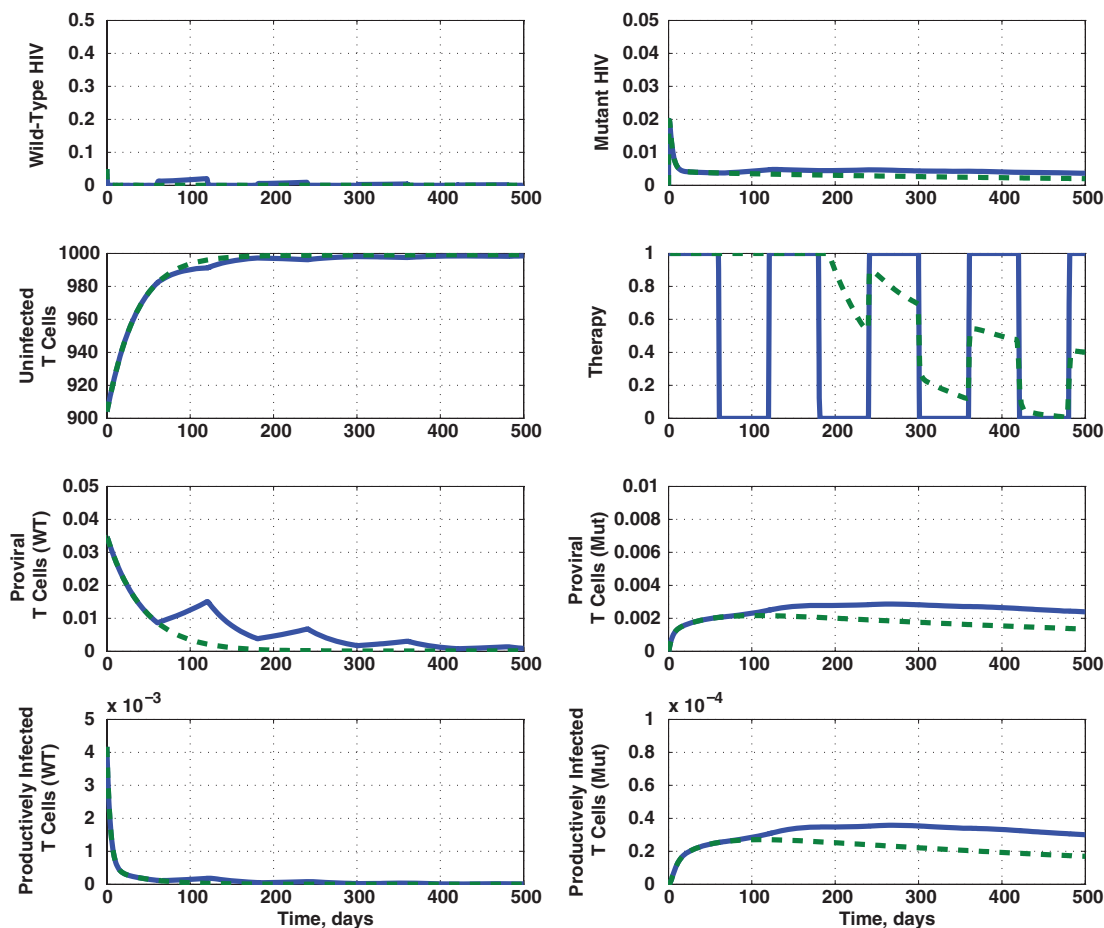
Fig. 8. Effect of periodic therapy on viral concentrations and immune response. Mutant fitness = 60%. 60-day period (solid line), partially optimized therapy initialized with periodic therapy (dashed line).

T_h cell infection responds as well; however, the mutant populations are not diminished but are higher than for the optimal case (dashed lines of Fig. 7). Using the periodic therapy as a starting point, 20 iterations of the optimizing algorithm produce the dashed curves of Fig. 8. The response is improved with partial optimization, demonstrating that the periodic therapy has no benefit.

There is a major caveat: we have no control over the fitness of mutant strains, and there is every reason to believe that mutations at every fitness level occur. Nevertheless, the present results suggest that monotherapy can have an effect on controlling at least some proportion of the drug-resistant mutant population. Multi-drug therapy targets different mutant strains, increasing overall efficacy. If fitness, drug resistance, and progression of the disease are related, as suggested in [10,46], optimizing multi-drug strategies may reveal synergistic effects that are currently unknown, providing better control of the virus and reducing harmful side effects of treatment.

3. Reflections and extensions

The suggestions for HIV therapy that are presented here are optimal only to the extent that the mathematical models are accurate reflections of host–pathogen–pharmaceutical interactions. Complex issues of pharmacokinetics have not been addressed, under the assumption that prescribed levels of therapeutic agents could be maintained in circulatory and lymphatic systems. The circulatory and lymphatic systems have been treated as a single control volume, although we know that host–pathogen interactions

and residence times are quite different in the periphery and in various lymphoid and mucosal tissues. Furthermore, no two individuals respond to infection and treatment in quite the same way, in large part because the rest of the body's systems couple into HIV response. The immune system's active response is only inferred in the model, the dynamics of CD4 cells other than T_h cells have been neglected, and details of viral reservoirs remain to be determined. There may never be answers to reasonable questions about the nature of important physiological traits and the potential direct and side effects of therapy.

Still, there is cause for future work on optimal therapies for HIV. Results of optimization provide a basis for rational design of therapies for trials and clinical application. The present analysis presumes that the therapy is derived from a single optimization over a fixed time interval, with known initial conditions, and with a perfect mathematical model. Robustness of the therapy can be increased by feedback control and state estimation. Because the time for computation is short compared to the time for treatment, the therapy could be derived and applied in a step-wise fashion from optimizations that were repeated on a periodic basis (e.g., every few weeks) using a current set of measurements, revisions to the model (if known), and a sliding end time. This is a nonlinear process known as *model predictive control* [48], a form of which is applied to HIV in [43]. References 49 and 50 present linear control alternatives to dealing with uncertainty and incompleteness in immune system models, measurements, and control action. Feedback control adjusts drug dosage to account for measured deviations of viral and immune response from optimal values [49], while state

estimation reduces the effects of feedback measurement and model errors [50]. In the normal course of biomedical research, models will improve, allowing control theory to make significant contributions to clinical practice.

4. Conclusion

Numerical optimization of nonlinear models can suggest improved therapies for treating HIV infection. The dynamics of infection are more complex and varied than portrayed by the simple mathematical models used here, but the analytical results give structures and rationales for treatment that could prove foundational for future practice. In particular, the study shows that current drug classes can provide indirect control of low-fitness drug-resistant HIV strains through dynamic coupling to wild-type strains and immune system dynamics. Current computational results support conclusions derived from clinical experience that "hit early, hit hard" therapy is optimal. Extension of this approach to multi-drug HIV therapy is straightforward and is the logical next step.

References

[1] R.C. Gallo, L. Montagnier, AIDS in 1988, Sci. Am. 259 (1988) 41.
[2] R.A. Weiss, How does HIV cause AIDS?, Science 260 (1993) 1273
[3] M. DiMascio, R.M. Ribeiro, M. Markowitz, D.D. Ho, A.S. Perelson, Modeling the long-term control of viremia in HIV-1 infected patients treated with antiretroviral therapy, Math. Biosci. 188 (2004) 47.
[4] J.G. Bartlett, R.D. Moore, Improving HIV therapy, Sci. Am. 279 (1998) 84.
[5] J. Salk, P.A. Bretscher, P.L. Salk, M. Clerici, G.M. Shearer, A strategy for prophylactic vaccination against HIV, Science 260 (1993) 1270.
[6] D.C. Douek, L.J. Picker, R.A. Koup, T cell dynamics in HIV-1 infection, Ann. Rev. Immunol. 21 (2003) 265.
[7] D.D. Ho, Time to hit HIV, hard and early, N. Engl. J. Med. 333 (1995) 450.
[8] D.D. Richman, HIV chemotherapy, Nature 410 (2001) 995.
[9] J.D. Watson, T.A. Baker, S.P. Bell, A. Gann, M. Levine, R. Losick, Molecular Biology of the Gene, Pearson/Benjamin Cummings, San Francisco, 2004.
[10] M.E. Quiñones-Mateu, E.J. Arts, HIV-1 fitness: implications for drug resistance, disease progression, and global epidemic evolution, HIV Sequence Compendium, Los Alamos National Laboratory, Los Alamos, NM (2001) 134.
[11] V. Joly, P. Yeni, Non nucleoside reverse transcriptase inhibitors, AIDS Rev. 1 (1) (1999) 37.
[12] B.C. Ciancio, M.P. Trotta, P. Lorenzini, F. Forbici, U. Visco-Comandini, C. Gori, S. Bonfigli, M.C. Bellohi, P. Sette, R. D'Arrigo, V. Tozzi, M. Zaccarelli, E. Boumis, P. Narciso, C.F. Perno, A. Antinoni, The effect of number of mutations and of drug-class sparing on Virological response to salvage genotype-guided antiretroviral therapy, Antivir. Ther. 8 (6) (2003) 611.
[13] W.E. Evans, H.L. McLeod, Pharmacogenomics – drug disposition, drug targets, and side effects, N. Engl. J. Med. 348 (2003) 538.
[14] D.C. Douek, P.D. Kwong, G.J. Nabel, The rational design of an AIDS vaccine, Cell 124 (2006) 677.
[15] D.J. Covert, D. Kirschner, Revisiting early models of the host–pathogen interactions in hiv infection, Comments Theor. Biol. 5 (6) (2000) 383.
[16] L. Cooper, Theory of an immune system retrovirus, Proc. Natil. Acad. Sci. USA 83 (1986) 9159.
[17] M.A. Nowak, R.M. May, R.E. Phillips, S. Rowland-Jones, D.G. Lalloo, S. McAdam, P. Klenerman, Köppe, K. Sigmund, C.R.M. Bangham, A.J. McMichael, Antigenic oscillations and shifting immunodominance in HIV-1 infections, Nature 375 (1995) 606.
[18] A.S. Perelson, P. Essunger, Y. Cao, M. Vesanen, A. Hurley, K. Saksela, M. Markowitz, D.D. Ho, Decay characteristics of HIV-1-infected compartments during combination therapy, Nature 387 (1997) 188.
[19] S.H. Bajaria, G. Webb, M. Cloyd, D. Kirschner, Dynamics of naïve and memory CD4$^+$ T lymphocytes in HIV-1 disease progression, J. Acquir. Immune Defic. Syndr. 30 (1) (2002) 41.
[20] P. Ye, A. Kourtis, D. Kirschner, The effects of different HIV type 1 strains on human thymic function, AIDS Res. Hum. Retrovirsues 18 (7) (2002) 1239.
[21] R.J. de Boer, A.S. Perelson, Target cell limited and immune control models of HIV infection: a comparison, J. Theor. Biol. 190 (1998) 201.
[22] D. Wodarz, A.L. Lloyd, V.A.A. Jansen, M.A. Nowak, Dynamics of macrophage and T cell infection by HIV, J. Theor. Biol. 196 (1999) 101.
[23] L.E. Jones, A.S. Perelson, Opportunistic infection as a cause of transient viremia in chronically infected HIV patients under treatment with HAART, Bull. Math. Biol. 67 (2005) 1227.
[24] M.A. Nowak, S. Bonhoeffer, G.M. Shaw, R.M. May, Anti-viral drug treatment: dynamics of resistance in free virus and infected cell population, J. Theor. Biol. 184 (1997) 203.
[25] L.M. Wein, R.M. D'Amato, A.S. Perelson, Mathematical analysis of antiretroviral therapy aimed at HIV-1 eradication or maintenance of low viral loads, J. Theor. Biol. 192 (1998) 81.
[26] S.H. Bajaria, G. Webb, D.E. Kirschner, Predicting differential responses to structured treatment interruptions during HAART, Bul. Math. Biol. 66 (5) (2004) 1093.
[27] N. Dixit, A.S. Perelson, Complex patterns of viral load decay under antiretroviral therapy; influence of pharmacokinetics and intracellular delay, J. Theor. Biol. 226 (2004) 95.
[28] L.E. Jones, A.S. Perelson, Modeling the effects of vaccination on chronically infected hiv-positive patients, J. Acquir. Immune Defic. Syndr. 31 (2002) 369.
[29] A.S. Perelson, Modeling the interaction of the immune system with HIV, in: C. Castillo-Chavez (Ed.), Mathematical and Statistical Approaches to AIDS Epidemiology, Springer-Verlag, New York, 1989, p. 50.
[30] A.S. Perelson, D.E. Kirschner, R.J. DeBoer, Dynamics of HIV infection of CD4$^+$ T cells, Math. Biosci. 114 (1993) 81.
[31] X. Wei, S.K. Ghosh, M.E. Taylor, V.A. Johnson, E.A. Emini, P. Deutsch, J.D. Lifson, S. Bonhoeffer, M.A. Nowak, B.H. Hahn, M.S. Saag, G.M. Shaw, Viral dynamics in human immunodeficiency virus type 1 infection, Nature 373 (1995) 117.
[32] D.D. Ho, A.V. Neumann, A.S. Perelson, W. Chen, J.M. Leonard, M. Markowitz, Rapid turnover of plasma virions and CD4 lymphocytes in HIV-1 infection, Nature 373 (1995) 123.
[33] A.S. Perelson, A.V. Neumann, M. Markowitz, J.M. Leonard, D.D. Ho, HIV-1 dynamics in vivo: virion clearance rate, infected cell life-span, and viral generation time, Science 271 (1996) 1582.
[34] A.S. Perelson, P.W. Nelson, Mathematical analysis of HIV-1 dynamics in vivo, SIAM Rev. 41 (1) (1999) 3.
[35] D.S. Callaway, A.S. Perelson, HIV-1 infection and low steady state viral loads, Bull. Math. Biol. 64 (2002) 29.
[36] J.A. Garcia, L.E. Soto-Ramirez, G. Cocho, T. Govezensky, M.V. José, HIV-1 dynamics at different time scales under antiretroviral therapy, J. Theor. Biol. 238 (2006) 220.
[37] M.S. Ciupe, B.L. Bivort, D.M. Bortz, P.W. Nelson, Estimating kinetic parameters from HIV primary infection data through the eyes of three different mathematical models, Math. Biosci. 200 (2006) 1.
[38] D. Kirschner, S. Lenhart, S. Serbin, Optimal control of the chemotherapy of HIV, J. Math. Biol. 35 (1997) 775.
[39] M.E. Brandt, G. Chen, Feedback control of a biodynamical model of HIV-1, IEEE Trans. Biomed. Eng. 48 (7) (2001) 754.
[40] S.J. Snedecor, Comparison of three kinematic models of HIV-1 infection: implications for optimization of treatment, J. Theor. Biol. 221 (2003) 519.
[41] R.L. Culshaw, S. Ruan, R.J. Spiteri, Optimal HIV treatment by maximising immune response, J. Math. Biol. 48 (2004) 542.
[42] S.S. Ge, Z. Tian, T.H. Lee, Nonlinear control of a dynamic model of HIV-1, IEEE Trans. Biomed. Eng. 52 (3) (2005) 353.
[43] R. Zurakowski, A.R. Teel, A model predictive control based scheduling method for HIV therapy, J. Theor. Biol. 238 (2006) 368.
[44] R.F. Stengel, Optimal Control and Estimation, Dover Publications, New York, 1994.
[45] R.F. Stengel, R. Ghigliazza, N. Kulkarni, O. Laplace, Optimal control of innate immune response, Optimal Control Appl. Methods 23 (2002) 91.
[46] M.A. Nowak, R.M. May, Virus Dynamics, Oxford University Press, Oxford, 2000.
[47] L.K. Doepel, International HIV/AIDS Trial Finds Continuous Antiretroviral Therapy Superior to Episodic Therapy. NIH News, National Institutes of Health. Available from: http://www.nih.gov/news/pr/jan2006/niaid-18.htm, Jan. 18, 2006.
[48] D. Mayne, J. Rawlings, C. Rao, P. Scokaert, Constrained model predictive control: stability and optimality, Automatica 36 (2000) 789.
[49] R.F. Stengel, R. Ghigliazza, N. Kulkarni, Optimal enhancement of immune response, Bioinformatics 18 (9) (2002) 1227.
[50] R.F. Stengel, R. Ghigliazza, Stochastic optimal enhancement of immune response, Math. Biosci. 191 (2004) 123.